BIOORGANIC CHEMISTRY 4, 136–148 (1975)

Multifunctional Hydrolytic Catalysis
II. Hydrolysis of *p*-Nitrophenyl Acetate by a Polymer Catalyst Which Contains Hydroxamate and Imidazole Functions[1]

TOYOKI KUNITAKE AND YOSHIO OKAHATA

Department of Organic Synthesis, Faculty of Engineering, Kyushu University, Fukuoka, 812, Japan

Received September 30, 1974

A water-soluble polymer catalyst was prepared by radical polymerization of a protected hydroxamate monomer, 1-methyl-2-vinylimidazole and acrylamide, and by the subsequent NH_2NH_2 treatment of the polymer. The hydrolysis of *p*-nitrophenyl acetate by the bifunctional copolymer obeyed typical burst kinetics: rapid accumulation of acetyl hydroxamate group and its slow decomposition. The acetylation rate of the hydroxamate group was rather close to that of a polymer which does not contain the imidazole unit. However, the deacylation was markedly accelerated by the presence of the imidazole unit, and the difference in rate constants amounted to 60- to 80-fold at pH 8–9. These results indicate that the overall catalytic efficiency of the bifunctional polymer is enhanced due to the complementary action of the imidazole and hydroxamate functions.

INTRODUCTION

The present paper describes the catalytic hydrolysis of *p*-nitrophenyl acetate by a copolymer containing the hydroxamate and imidazole functions. The hydroxamate anion is known to be highly nucleophilic toward phenyl esters (*1–6*), and the nucleophilicity becomes even greater when substrate binding is possible (*7, 8*). However, the true catalytic efficiency of this functional group in the hydrolysis of phenyl esters is in general limited because of the slow decomposition of the acyl hydroxamate intermediate. This behavior was also true in a polymeric system, as we showed recently (*9*). The catalytic efficiency may be made greater by introduction of suitable functional groups which are capable of accelerating the deacylation process. For instance, Gruhn and Bender showed that an intramolecular tertiary amino group accelerated the hydrolysis of an acetyl hydroxamate intermediate (*10*). For the same purpose, we prepared a water-soluble copolymer containing the hydroxamate and imidazole functions and examined its catalytic efficiency in the hydrolysis of *p*-nitrophenyl acetate (PNPA), in comparison with that of a copolymer containing the hydroxamate function alone. This system is of particular interest as a model system of the active site of serine esterases.

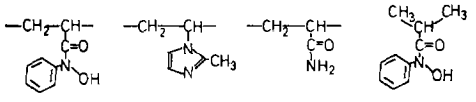

[1] Contribution No. 347 from this department. A preliminary description of the present study has been published: T. Kunitake, Y. Okahata, and R. Ando, *Macromolecules*, 7, 140 (1974).

EXPERIMENTAL

Materials

Acetyl *N*-phenylacrylohydroxamate (acetyl-PHA), *N*-phenylisobutyrohydroxamic acid (model PHA) and its *O*-acetyl derivative, acrylamide (AAm), and *p*-nitrophenyl acetate (PNPA) were prepared and/or purified as described before (*9*). 1-Vinyl-2-methylimidazole (MIm), as provided by Toho Rayon Co., was distilled: bp 88–88.5°C/15 mm Hg.

Copolymerization

The copolymerization of acetyl-PHA and acrylamide was described previously (*9*). The copolymerization of 1-vinyl-2-methylimidazole and acrylamide was carried out in methanol with AIBN initiator, and the polymer was reprecipitated from methanol and ether. The ternary copolymerization of acetyl-PHA, 1-vinyl-2-methylimidazole, and acrylamide was conducted in acetonitrile or benzene. The precipitated polymer was collected, dissolved in dry methanol, and poured into ether or acetone. All the polymer samples were dried *in vacuo* and weighed. The polymerization results are summarized in Table 1.

TABLE 1

COPOLYMERIZATION

Run No.	Monomer feed			Time (min)	Conversion (wt %)	Composition (mole %)		
	acetyl-PHA (*M*)	MIm (*M*)	AAm (*M*)			PHA	MIm	AAm
1[a]	0.10	—	0.90	10	22	10	—	90[d]
2[a]	0.05	0.95	—	135	30	11	89	—
3[b]	—	2.40	1.60	15	30	—	36	64[e]
4[b]	0.25	2.40	1.36	90	40	10	62	28[f]
5[c]	0.05	0.80	0.15	40	40	3	60	37[d]
6[c]	0.05	0.10	0.85	10	28	3	7	90[d]

[a] 80°C, CH_3CN solvent, AIBN 0.02 *M*.
[b] 70°C, MeOH solvent, AIBN 0.02 *M*.
[c] 70°C, benzene solvent, AIBN 0.02 *M*.
[d] Determined by nmr and uv methods.
[e] Determined by potentiometric titration.
[f] Determined by uv and nmr spectroscopy and by potentiometric titration.

Deacylation

An aqueous solution of the acetyl–PHA–AAm copolymer was treated with NH_2OH as described before, and the polymer was recovered by pouring into excess methanol and dried *in vacuo*: recovery 95%. In the case of the terpolymer (run. No. 4, Table 1), the acetyl polymer was dissolved in wet methanol and allowed to react with excess hydrazine hydrate at room temperature with stirring. After 24 hr the solution was added to excess acetonitrile or acetone. The reprecipitation was repeated and the polymer dried *in vacuo*: polymer recovery 90%. Completion of deacetylation was confirmed by disappearance of an ir peak of the actyl hydroxamate group (1800 cm^{-1}).

Copolymer Composition

The composition of the deacylated copolymer (PHA–AAm) was determined by nmr spectroscopy and by the uv titration of the hydroxamate group as described before. The content of the imidazole unit in the MIm–AAm copolymer was determined by the potentiometric titration. The composition of the PHA–MIm–AAm terpolymer was determined by a combination of the potentiometric titration and uv and nmr spectroscopies. In the potentiometric titration, the PHA and MIm groups cannot be titrated separately, and their combined contents are obtained. Similarly, the nmr spectroscopy gives the combined content from the relative peak area of the aromatic and aliphatic protons. The PHA content can be estimated from uv spectroscopy by using *N*-phenylisobutyrohydroxamic acid as a model compound: $\varepsilon = 2020$ at 300 nm in 28.9 v/v% EtOH–H_2O, 0.01 *N* NaOH.

Copolymers PHA–MIm and PHA–MIm–AAm-5, were not soluble in 28.9 v/v% EtOH–H_2O. Their compositions were determined by the nmr and uv methods.

Determination of pK_a

The pK_a value of the PHA unit was determined from the uv absorption difference between the hydroxamate anion ($\varepsilon = 2020$ at 300 nm in 0.01 *N* NaOH) and the hydroxamic acid ($\varepsilon = 30$ at 300 nm in 0.01 *N* HCl) at several pH's. The medium was 28.9 v/v% EtOH–H_2O, 0.1 *M* KCl, 0.15 *M* barbital buffer, 30°C. The MIm and AAm units do not absorb in this region. The pK_a value of the MIm group was determined by the potentiometric titration: 30°C, 28.9 v/v% EtOH–H_2O, 0.1 *M* KCl.

The titration data were plotted according to the modified Henderson-Hasselbach equation (*11*)

$$pK_a = pH + n' \log \frac{1-\alpha}{\alpha}, \tag{1}$$

where α is the fraction of the dissociated hydroxamic acid group or of the neutral imidazole species.

The titration results are shown in Table 2, together with the polymer composition.

TABLE 2

COPOLYMERS

Polymer	Composition (mole %) PHA	MIm	AAm	Functional group	Titration[a] pK_a	n'	pK_{int}[b]	$[\eta]$[c]
PHA–MIm–AAm-4	10	62	28	PHA	9.24	1.33	8.96	0.05
				MIm	6.60	1.64	7.22	
PHA–AAm	10	—	90	PHA	9.12	1.45	8.72	0.32
MIm–AAm	—	36	64	MIm	6.34	1.46	6.78	—

[a] 30°C, 0.1 *M* KCl, 28.9 v/v% EtOH–H_2O. The titrations of the PHA and MIm units were done by uv and potentiometric methods, respectively.

[b] pK_{int} is the limiting pK_a value at zero dissociation.

[c] 30°C, 1 *M* aqueous KCl.

Rate Measurements

The time course of the reaction of PNPA with polymers and with *N*-phenylisobutyrohydroxamic acid was followed by measuring the release of the *p*-nitrophenolate anion at 401 nm. The hydrolysis of acetyl hydroxamate groups was followed by using the absorption of the hydroxamate anion formed at 300 nm. The reaction condition was as follows in all cases: 30°C, 28.9 v/v% EtOH–H_2O, 0.1 *M* KCl, 0.05–0.15 *M* barbital buffer. The pH value of the reaction medium was ascertained not to change (the fluctuation less than 0.02 pH unit) during the course of reaction from the pH measurements before and after the reaction.

In the burst kinetics, 0.094-cm pathlength was employed because the substrate concentration was high. A typical procedure is as follows: Stock solutions of PNPA in dry ethanol and of catalyst in H_2O are prepared. In a 1-cm cell is added 390 μl of a buffer solution (25 v/v% EtOH–H_2O) and a necessary amount of the catalyst stock solution. Ethanol and water are added when necessary, so that the total volumes of EtOH and H_2O added are 40 and 20 μl, respectively, apart from the buffer solution. The cell is shaken and placed in a thermostatted cell holder. A spacer (0.906-cm path) is also put in the reference cell. After 5 min, a required amount (10–40 μl) of the substrate solution is added, the cell shaken, and the spacer inserted into the sample cell. The recorder is started simultaneously. Care must be taken so that there is no bubble formation between the cell wall and spacer. The total volume of the reaction mixture is 450 μl. The spontaneous hydrolysis is carried out in the same way except for the addition of the catalyst solution.

Essentially the same procedure was employed when a 1.0-cm cell was used without a spacer. The total volume of the reaction mixture in this case was 3.32 ml.

Miscellaneous

All the uv measurements were made with a Hitachi 124 uv-visible spectrometer equipped with a thermostatted cell compartment. A Toa digital pH meter (Model HM-15A) was employed for the pH measurement, and a Toa pH stat system was used for the potentiometric titration. The viscosity of polymers was obtained by using a modified Ubbelohde viscometer. The reaction rate was calculated by using a programmable desk calculator Compet 364P. The least-squares method was used wherever possible. The correlation coefficient was better than 0.99 unless stated otherwise.

RESULTS

Hydrolysis of PNPA by PHA–MIm–AAm Polymer

The release of the *p*-nitrophenolate anion consists of the catalytic and spontaneous terms

$$v_{\text{total}} = v_{\text{cat}} + v_{\text{spont}}. \tag{2}$$

The reaction of PHA–MIm–AAm with large excesses of PNPA gives typical burst kinetics; i.e., the initial rapid liberation of *p*-nitrophenol followed by the slower, steady release. An example is shown in Fig. 1. This curve was obtained by subtracting the phenol release due to spontaneous hydrolysis from the overall release. These

experiments with and without the polymer catalyst were always conducted consecutively, in order to minimize the experimental error. This result is in sharp contrast with the reaction of the PHA–AAm polymer and PNPA which is carried out under the same reaction conditions. In this case, the secondary phenol release was too slow to determine the reaction rate.

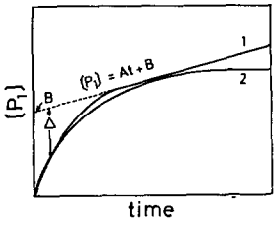

FIG. 1. Burst kinetics: (1) for PHA–MIm–AAm-4; (2) for PHA–AAm.

The analysis of the burst kinetics of simple nucleophilic esterolysis has been reported by Bender et al. (*12*). The nucleophilic catalysis of the ester hydrolysis is expressed by

$$\begin{matrix} C + S \xrightarrow{k_a} CS' \xrightarrow{k_d} C + P_2, \\ + \\ P_1 \end{matrix} \tag{3}$$

where C, S, and CS′ denote catalyst, ester substrate, and acyl intermediate, respectively. When the second step is slow relative to the first step and if [S] ≫ [C], rapid liberation of P_1 and accumulation of CS′ are observed. The rate of formation of P_1 is given by

$$\frac{dP_1}{dt} = a - \frac{ak_a[S]_0}{b}(1 - e^{-bt}), \tag{4}$$

where

$$a = k_a[C]_0[S]_0, \tag{5}$$

$$b = k_a[S]_0 + k_d. \tag{6}$$

By integration and substitution we obtain

$$[P_1] = At + B(1 - e^{-bt}), \tag{7}$$

where

$$A = a - (a/b)k_a[S]_0, \tag{8}$$

$$B = (a/b^2)k_a[S]_0. \tag{9}$$

Δ is defined as the difference in the phenol release between the dotted line (extrapolation of the linear portion) and the burst curve:

$$\Delta = Be^{-bt}. \tag{10}$$

Thus the B and b values are obtained from the linear plot of $\log B$ and t, and the k_a and k_d values are determined from the following equations:

$$k_a = \frac{b\sqrt{B}}{[S]_0([C]_0)^{1/2}}, \tag{11}$$

$$k_d = b - k_a[S]_0. \tag{12}$$

In the present catalytic system, two kinds of nucleophilic function—hydroxamate and imidazole—are present, and both of these functions are responsible for the formation of P_1 (*p*-nitrophenol). However, the *p*-nitrophenol release due to the MIm unit is much slower than that due to the PHA unit, as shown below. Therefore, the Bender procedure was employed without modification.

In Table 3 are given some kinetic constants determined by the above-mentioned analysis of the burst kinetics at different substrate concentrations. The $k_{a,\,obs}$ and $k_{d,\,obs}$ values were calculated from Eqs. (11) and (12) for each substrate concentration.

TABLE 3

BURST KINETICS[a]

Run No.	[PNPA] ($\times 10^4$ *M*)	[PHA] ($\times 10^4$ *M*)	b[b]	B[b] ($\times 10^4$ *M*)	$k_{a,\,obs}$[c] (M^{-1} sec^{-1})	$k_{d,\,obs}$[d] ($\times 10^3$ sec^{-1})
1	105	6.33	0.0362	5.04	3.21	1.53
2	92.3	6.33	0.0311	5.40	3.11	2.37
3	79.1	6.33	0.0240	5.38	2.79	1.86
4	65.9	6.33	0.0227	5.50	3.21	1.53

[a] Catalyst: PHA–MIm–AAm-4, pH = 8.93, 28.9 v/v% EtOH–H_2O, 30°C, 0.1 *M* KCl, 0.15 *M* barbital.

[b] Calculated from logarithmic plot of Eq. (10).

[c] Calculated from Eq. (11).

[d] Calculated from Eq. (12).

The b value as obtained from the logarithmic plot of Eq. (10) was plotted against the substrate concentration. A linear relation was found in accordance with Eq. (6). The $k_{a,\,obs}$ and $k_{a,\,obs}$ values determined from this linear relationship ($r = 0.98$) were 3.11 M^{-1} sec^{-1} and 1.86×10^{-3} sec^{-1}, respectively, in satisfactory agreement with those determined from Eqs. (11) and (12) without changing the substrate concentration.

The k_a and k_d values may also be determined by using the slope of the linear portion [cf. Eq. (8)]. However, the slope was very small, and the kinetic constants thus obtained, in particular $k_{d,\,obs}$ values, were unreliable compared with those calculated from the initial burst portion.

The $k_{a,\,obs}$ and $k_{d,\,obs}$ values were similarly determined from the burst reactions at several other pH's and are summarized in Table 4. These rate constants are given for the total PHA concentration. The $k_{a,\,obs}$ value increases with increasing pH, reflecting the increasing amount of the hydroxamate anion.

It must be mentioned that large errors tend to be involved in the determination of $k_{d,\,obs}$ values, caused by the fact that the turnover of the catalytic site is not much faster than the spontaneous hydrolysis. Thus, kinetic data were discarded when the $k_{a,\,obs}$ value calculated was not reasonable.

The burst experiment was also carried out with other terpolymer catalysts like PHA–MIm–AAm-6 (Table 1, No. 6). However, the deacylation process was barely observable in this case, because the MIm content was small (7%) relative to PHA–MIm–AAm-4 (MIm content 62%).

TABLE 4

BURST KINETICS[a]

pH	Barbital (M)	$k_{a,\,obs}$[b] (M^{-1} sec^{-1})	$k_{d,\,obs}$[c] ($\times 10^3$ sec^{-1})	α_{PHA}[d]
9.12	0.15	2.90	4.35	0.448
9.12	0.15	2.65	4.31	0.448
8.98	0.15	1.73	2.92	0.389
8.76	0.075	1.03	2.39	0.303
8.76	0.075	1.29	1.55	0.303
8.62	0.075	1.01	1.98	0.255
8.42	0.075	0.50	1.02	0.209
8.32	0.15	0.68	1.05	0.169
8.15	0.10	0.38	0.45	0.132
8.01	0.075	0.34	0.54	0.106

[a] 30°C, 28.9 v/v% EtOH–H_2O, 0.1 M KCl, barbital buffer. [PNPA] = 1.12×10^{-2} M; [PHA] = 6.60×10^{-4} M.
[b] Calculated from Eq. (11).
[c] Calculated from Eq. (12).
[d] pH = $-1.33 \log [(1 - \alpha)/\alpha] + 9.24$.

Acylation of the Hydroxamate Group with PNPA

The reactions of PHA–AAm copolymer and *N*-phenylisobutyrohydroxamic acid (model PHA) with PNPA were conducted in 28.9 v/v% EtOH–H_2O under the pseudo-first-order condition: i.e., excess hydroxamic acid. The same reaction was carried out previously in 1.4 v/v% CH_3CN–H_2O (*9*). The overall pseudo-first-order rate constant ($k_{overall}$) was determined from the first-order plot of $\log[(OD_\infty - OD_0)/(OD_\infty - OD_t)]$ vs time and corrected for spontaneous hydrolysis: $k_{a,\,obs}[PHA]_0 = k_{overall} - k_{spont}$. These results are summarized in Table 5. The $k_{a,\,obs}$ value for the model PHA compound increases, as expected, in proportion to the fraction of the dissociated hydroxamic acid, whereas this is not the case for the polymer (see below).

TABLE 5

ACYLATION OF THE HYDROXAMATE GROUP BY PNPA[a]

PHA–AAm[b]		Model PHA[c]	
pH	$k_{a,\,obs}$ (M^{-1} sec^{-1})	pH	$k_{a,\,obs}$ (M^{-1} sec^{-1})
9.10	3.66	9.09	5.77
8.93	2.95	8.94	4.49
8.64	2.11	8.66	3.02
8.45	1.38	8.47	1.78

[a] 28.9 v/v% EtOH–H_2O, 30°C, 0.1 M KCl, 0.15 M barbital, [PNPA] = 4.12×10^{-5} M.
[b] [PHA] = 5.52×10^{-4} M.
[c] [PHA] = 5.97×10^{-4} M.

Hydrolysis of Acetyl Hydroxamates

The hydrolysis of acetyl *N*-phenylisobutyrohydroxamate and the acetylated PHA–AAm polymer were carried out at three different barbital concentrations (0.05, 0.10, and 0.15 *M*). The apparent rate constants were determined from the first-order plot and extrapolated to the zero buffer concentration. The apparent rate constant of deacylation increases with decreasing concentrations of barbital. This is contrary to the trend observed in Tris buffer (*9*). The $k_{d,\,obs}$ values at the zero buffer concentration are summarized in Table 6. The rate constants for the hydroxide and water hydrolyses were calculated from these data and are listed in Table 6. It must be mentioned that the $k_{d,\,obs}$ value determined from the burst kinetics are not extrapolated to the zero buffer concentration. However, the correction due to barbital buffer was in the range of $(1\text{–}5) \times 10^{-5}$ sec^{-1} for the hydrolysis of simple and polymeric acetyl hydroxamates. Therefore, the possible error involved would be small.

TABLE 6

DEACETYLATION[a]

Compound	pH	$k_{d,\,obs}$[b] ($\times 10^5$ sec^{-1})	k_{OH} (M^{-1} sec^{-1})	k_{H_2O} ($\times 10^5$ sec^{-1})
Acetylated model PHA	9.19	5.33	1.80	0.9
	9.31	6.48		
	9.52	10.9		
Acetyl-PHA–AAml	9.22	9.80	3.2	0
	9.38	11.6		
	9.58	19.1		

[a] 28.9 v/v% EtOH–H_2O, 30°C, 0.1 *M* KCl, 0.05–0.15 *M* barbital buffer.

[b] Obtained by extrapolation to the zero buffer concentration. $k_{d,\,obs} = k_{OH}[OH^-] + k_{H_2O}$.

Hydrolysis by MIm–AAm Polymer

The hydrolysis of PNPA by the MIm–AAm polymer was carried out in the presence of a large excess of the MIm unit, and the second-order rate constant $k_{a,\,obs}$ was determined by the Guggenheim plot of the pseudo-first-order reaction (Table 7). The $k_{a,\,obs}$

TABLE 7

HYDROLYSIS OF PNPA BY MIm–AAm[a]

pH	$k_{overall}$ ($\times 10^4$ sec^{-1})	k_{spont} ($\times 10^4$ sec^{-1})	$k_{a,\,obs}$ ($\times 10^3$ M^{-1} sec^{-1})
8.78[b]	1.51	1.26	1.58
7.85[c]	1.64	1.43	1.33

[a] 30°C, 28.9 v/v% EtOH–H_2O, 0.1 *M* KCl, [PNPA] = 6.29×10^{-5} *M*, [MIm] = 1.58×10^{-3} *M*.

[b] Barbital buffer 0.15 *M*.

[c] Tris buffer 0.15 *M*.

value for the MIm unit is smaller than those of the PHA unit by a factor of approximately 10^3. Accordingly, the acetyl-PHA–AAm polymer was hydrolyzed in the presence and absence of the MIm–AAm polymer. The results are summarized in Table 8. Apparently, the presence of 0.03–0.08 *M* of the MIm unit does not noticeably increase the $k_{d,\,obs}$ value. It is therefore concluded that only the intramolecular MIm unit accelerates the hydrolysis of the acetyl-PHA unit.

TABLE 8

HYDROLYSIS OF ACETYL-PHA–AAm BY MIm–AAm[a]

pH	[acetyl-PHA] ($\times 10^4$ *M*)	[MIm] ($\times 10^2$ *M*)	$k_{d,\,obs}$ ($\times 10^5$ sec^{-1})
9.38	7.47	—	11.5
9.36	7.47	3.51	11.6
9.17	8.52	—	2.68
9.17	8.52	8.00	2.65

[a] 30°C, 28.9 v/v% EtOH–H_2O, 0.1 *M* KCl, 0.15 *M* barbital.

DISCUSSION

The PHA–MIm–AAm polymer contains two kinds of nucleophilic functional groups, and both of them can catalyze the hydrolysis of active esters. Therefore, several possibilities arise as to the course of catalysis.

In the first place, the reaction of PNPA may occur at the PHA site and/or at the MIm site. The apparent rate constant of reaction of PNPA with the PHA unit and its small-molecule analog is much greater than that with the MIm unit: 0.5–3 M^{-1} sec^{-1} vs 1.5×10^{-3} M^{-1} sec^{-1}, meaning that the direct reaction of PNPA with the MIm unit is negligible in the case of the PHA–MIm–AAm polymer. Therefore, the first step in the catalysis is the acylation of the PHA unit, leading to the formation of the acetylated PHA unit and *p*-nitrophenol. The very observation of the burst kinetics for the PHA–MIm–AAm polymer is consistent with this conclusion. The hydrolysis of PNPA by the MIm unit alone would not give rise to the burst kinetics, as the acetylimidazole intermediate is not accumulated because of fast decomposition.

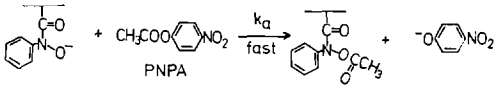

(13)

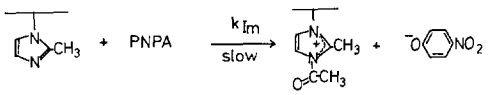

(14)

Figure 2 shows the dependence of the $k_{a,\,obs}$ value on the fraction of the dissociated hydroxamic acid group, α_{PHA}. The $k_{a,\,obs}$–α_{PHA} relation for the small-molecule hydroxamic acid is linear, consistent with the fact that the hydroxamate anion is the true

reacting species (*3–5*). On the other hand, the acylation of the PHA unit in polymer does not exhibit the linear dependency; instead, upward curvatures were observed. This kind of difference between the small-molecule and polymer systems was observed previously (*9*). The same explanation as presented in the previous paper seems to be applicable to the present results: The reactivity of a given hydroxamate anion is lessened because of its intramolecular aggregation with the undissociated PHA unit, and, as the degree of dissociation increases, the side-chain aggregation is destroyed by expansion of the polymer coil due to increasing electrostatic repulsion among the negatively charged groups.

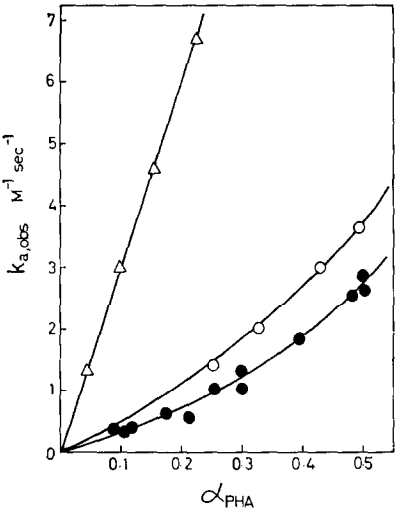

FIG. 2. Acylation of the hydroxamate group by PNPA. 30°C, 28.9 v/v% EtOH–H_2O, 0.1 *M* KCl 0.15 *M* barbital. △, model PHA; ○, PHA–AAm; ●, PHA–MIm–AAm-4.

There were observed very similar tendencies in both PHA–AAm and PHA–MIm–AAm copolymers, and, in addition, introduction of the MIm unit lowered the reactivity of the PHA anion. It appears that the MIm unit simply decreases the reactivity of the PHA unit because of increased hydrophobicity. Therefore, it may be concluded that these two functional groups participate in the catalytic process fairly independently.

The second stage in the catalytic action of the bifunctional polymer is the decomposition of the acetyl hydroxamate intermediate. The MIm unit must play an important role in deacylation of the PHA–MIm–AAm terpolymer, since the $k_{d,\,obs}$ value for this polymer is much greater than those for the PHA–AAm polymer and simple hydroxamic acids (Tables 4 and 6). The rate difference amounts to 60- to 80-fold at pH 8–9 (see Fig. 3). The effectiveness of imidazole in the hydrolysis of acetyl hydroxamates has been reported in the literature (*13*). As shown in Table 8, there was no detectable rate change in the deacylation of the PHA–AAm polymer when the MIm–AAm polymer was added. Therefore, the MIm unit in the same polymer chain is much more effective than that in other polymer molecules. In Fig. 3 are plotted $\log k_{d,\,obs}$ against pH. Linear relationships are observed for all the systems. Slopes for the hydrolysis of PNPA,

acetyl-PHA–AAm, and acylated model PHA are unity, reflecting the hydroxide hydrolysis. On the other hand, the terpolymer PHA–MIm–AAm gives a slope of less than unity. Although the linearity may be related to the logarithmic decrease of the positive charge in the polymer chain, appropriate explanations for the observed slope cannot be found.

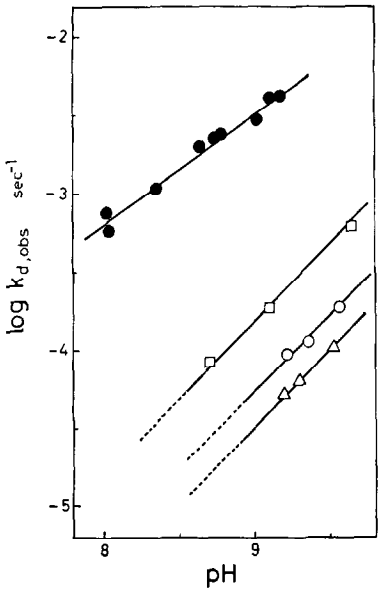

FIG. 3. Hydrolysis of acetyl-PHA units and PNPA. 30°C, 28.9 v/v% EtOH–H_2O, 0.1 *M* KCl. ●, PHA–MIm–AAm-4; ○, acetyl-PHA–AAm; △, acetylated model PHA; □, PNPA. The plots for PHA–MIm–AAm-4 were obtained at 0.15 *M* barbital. The others were obtained by extrapolation to the zero buffer concentration.

The imidazole group may catalyze deacylation in two ways. They are nucleophilic and general base catalyses. In the case of the nucleophilic catalysis, the acetyl group is transferred from the PHA site to the MIm site. The hydrolysis of the acetylated MIm unit completes the catalytic cycle (Eq. (15)). In general base catalysis, the MIm unit helps the H_2O attack the acetyl hydroxamate (Eq. (16)). At present it is not known which of these mechanisms is operating.

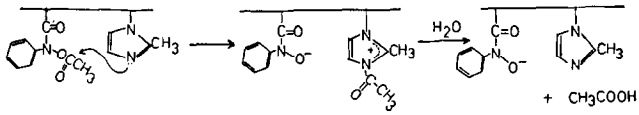

(15)

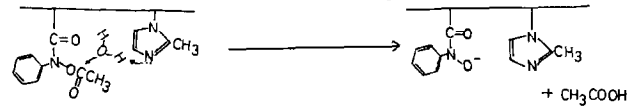

(16)

The deacylation reaction is effected by the intramolecular MIm unit in the PHA–MIm–AAm polymer. Then, the $k_{d,\,obs}$ value must be related to the availability of the

basic MIm group. Figure 4 is a plot of $k_{d,\,obs}$ vs the fraction of the neutral MIm unit, α_{MIm}, in the terpolymer. Interestingly, $k_{d,\,obs}$ shows a steep rise as α_{MIm} approaches unity. This result cannot be explained by simple availability of the neutral MIm unit. Linear dependency should be observed, if the availability of the neutral MIm unit alone is important.

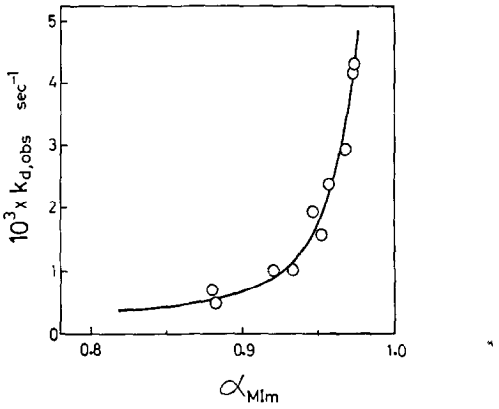

FIG. 4. Deacetylation of PHA–MIm–AAm-4. 30°C, 28.9 v/v% EtOH–H_2O, 0.1 *M* KCl, 0.15 *M* barbital.

It is expected that the polymer forms an increasingly tighter coil as the isoelectric point approaches. Figure 5 shows the pH variations of the amount of the charged unit (MIm^+ and PHA^-), which are calculated from the titration data. The isoelectric point is 8.73. The increase in $k_{d,\,obs}$ with pH, as shown in Fig. 3, may be explained by

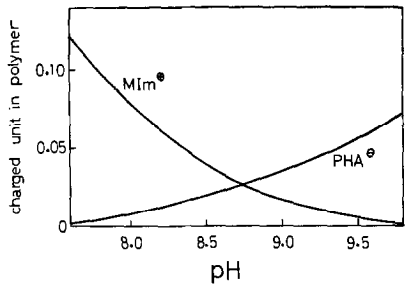

FIG. 5. Variation of the content of the charged units in PHA–MIm–AAm-4. $MIm^{\oplus}$: protonated MIm unit. $PHA^{\ominus}$: dissociated PHA unit. Solid curves were calculated from the copolymer composition and the degrees of dissociation. The charged unit contents are given relative to the total monomer unit.

the shrinkage of the polymer chain. It has been noted in several instances that the efficiency of polymer catalysts is highly dependent upon the extent of intramolecular aggregation. Overberger et al. (*14*) found that the rate of reaction of polyvinylimidazole and a long-chain phenyl ester varied dramatically with the solvent composition, and they explained this from the difference in polymer aggregation. Similarly, the assistance of deacylation by the neutral imidazole unit would be more efficient when a tighter polymer coil is formed.

In conclusion, it was shown in the present work that a combination of appropriate catalytic functions can enhance the overall catalytic efficiency. Since the deacylation process is rate limiting in the hydroxamate system, the overall catalytic efficiency increased 60–80 times by introduction of the MIm unit. Further increases in the catalytic efficiency are expected when different imidazole units and/or different arrangements of the hydroxamate and imidazole functions are used.

REFERENCES

1. H. KWART AND H. OMURA, *J. Org. Chem.*, **32**, 318 (1969).
2. J. D. AUBORT AND R. F. HUDSON, *Chem. Commun.*, 937 (1970); 938 (1970).
3. M. DESSOLIN, M. LALOI-DIARD, AND M. VILKAS, *Bull. Soc. Chim. Fr.*, 2573 (1970).
4. M. DESSOLIN AND M. LALOI-DIARD, *Bull. Soc. Chim. Fr.*, 2946 (1971).
5. M. DESSOLIN, *Tetrahedron Lett.*, 4585 (1972).
6. F. FILIPPINI AND R. F. HUDSON, *Chem. Commun.*, 522 (1972).
7. R. HERSFIELD AND M. L. BENDER, *J. Amer. Chem. Soc.*, **94**, 1376 (1972).
8. I. TABUSHI, Y. KURODA, AND S. KITA, *Tetrahedron Lett.*, 643 (1974).
9. T. KUNITAKE, Y. OKAHATA, AND R. ANDO, *Bull. Chem. Soc. Japan*, **47**, 1509 (1974).
10. W. B. GRUHN AND M. L. BENDER, *J. Amer. Chem. Soc.*, **91**, 5883 (1969).
11. A. KATCHALSKI, N. SHAVIT, AND H. EISENBERG, *J. Polym. Sci.*, **13**, 69 (1954).
12. M. L. BENDER AND T. H. MARSHALL, *J. Amer. Chem. Soc.*, **90**, 201 (1968).
13. J. F. KIRSCH AND W. P. JENCKS, *J. Amer. Chem. Soc.*, **86**, 837 (1964).
14. C. G. OVERBERGER AND M. MORIMOTO, *J. Amer. Chem. Soc.*, **93**, 3222 (1971).